

MOLECULAR DYNAMICS SIMULATION OF THE PRIMARY PROCESSES IN  
THE PHOTOSYNTHETIC REACTION CENTER OF *Rhodopseudomonas viridis*

H.Treutlein \*, K.Schulten \*, J.Deisenhofer †, H.Michel †,  
A.Brünger †, and M.Karplus †

\* Physik-Department, Technische Universität München  
D-8046 Garching, FRG

† Max-Planck-Institut für Biochemie, D-8033 Martinsried, FRG

† Department of Chemistry, Harvard University, Cambridge  
MA 02138, USA

ABSTRACT

We have carried out a computer simulation of the photosynthetic reaction center of *Rhodopseudomonas viridis* based on the available molecular structure<sup>1,2</sup>. Our simulation employed the CHARMM program<sup>3</sup> in conjunction with the so-called stochastic boundary method<sup>4</sup>. This method allowed us to study a functionally important segment of the photosynthetic reaction center with 3634 atoms, including the prosthetic groups involved in the primary electron transfer processes. Electron transfer has been modeled by re-charging the respective chromophores assuming charge distributions based on quantumchemical (MNDO) calculations. We discuss to which extent the protein matrix and chromophore arrangement control the relevant electron transfer steps.

1. INTRODUCTION

The main open question regarding the photosynthetic reaction center concerns the high efficiency with which an electron and a hole are separated by light absorption in the system and their recombination is being prevented. Three factors can contribute to this efficiency.

A first factor is the fast rate of the forward transfer of the electron after light excitation of the special pair. In order to understand this rate one needs to know which material properties of the reaction center are actually making the electron transfer possible.

A second factor contributing to the efficiency can be the electrostatic potential inside the reaction center which may favour the separation of electron and hole. In a second article<sup>5</sup> we consider in how far the electrostatic energy in the reaction center contributes in this respect.

A third factor contributing to the efficiency of the reaction center function lies in the fact that the time scales of back-transfer of the electron to the hole are much longer than the time scales for the forward transfers. In the following we will investigate control of electron transfer rates through mechanical motion of the chromophores

and their surrounding protein matrix which can either establish or hinder electrical contact. Since the time scale of the process under consideration, i.e. photoinduced electron transfer, is close to the time scale accessible to computer simulations of protein dynamics, the reaction center is an excellent candidate for a molecular dynamics study. In order to obtain an answer to the issues just raised we ask in our computer simulations the following key questions:

- What is the contribution of inherent atomic mobilities to electron transfer?
- How does the protein structure rearrange during electron transfer?
- What are the effects of 'site-directed mutagenesis' on the reaction center?

The last question also provides an important possibility for a comparison between experiments and theory.

## 2. METHOD

The simulations we describe in this article were based on the X-ray structure of the reaction center of *Rhodospseudomonas viridis* at 3 Å resolution<sup>1,2</sup>. The calculations involved the CHARMM program as described by B. R. Brooks et al.<sup>3</sup>. All charge distributions of the neutral and ionized chromophores have been calculated by means of the all valence electron MOPAC quantum chemistry program<sup>6</sup>.

The whole reaction center with more than 12000 atoms is actually too large to be handled within reasonable computer time by the simulation program. Therefore, we made use of the feature of CHARMM which by means of the method of stochastic boundaries allows to select a central part of the reaction center for the simulation. The selected part contained all chromophores except three heme units of the cytochrome. Since the selection has an important influence on the results, inducing actually some artifacts, we will briefly explain this method in the following.

The protein is divided into three disjunct sets of atoms. The first set, the *reaction region*, contains that region of the protein which one wants to describe in detail by the molecular dynamics method. For atoms in this region the deterministic Newtonian equations are integrated. Surrounding the reaction region is the *buffer region*. This region involves a shell of atoms which are described by Langevin molecular dynamics. For this purpose noise and friction is added to the Newtonian equations, these terms keeping the respective atoms at the proper temperature in order to prevent a cooling down of the atoms in the reaction region. In addition, a harmonic restoring force is added to the Newtonian equations which keeps the atoms in the buffer region on the average at their initial positions. The third region, the *reservoir region*, contains all other atoms. These atoms are completely neglected in the molecular dynamics description. Our choice of the three regions of the reaction center led us to include 3634 out of about 12000 atoms of the reaction center.

Figure 1 displays the chromophore structure inside the simulated protein segment (reaction and buffer region) together with their abbreviated names. Bonds between atoms inside the buffer region are marked by thick solid lines. Phytol chains of the non-functional branch chromophores (BCMP, which is part of the *special pair* dimer, BCMA and BPM) are partially located inside the buffer region, which implies that some of their atoms are constrained to their initial positions. This induces dynamical artifacts, that must be considered when trying to compare the dynamical properties between the functional (BCLP, the other chromophore of the *special pair*, BCLA, BPL, QA and the iron-ion FE1) and the non-functional chromophores. (Of the functional chromophores only a few atoms of the quinone QA lie inside the buffer region.

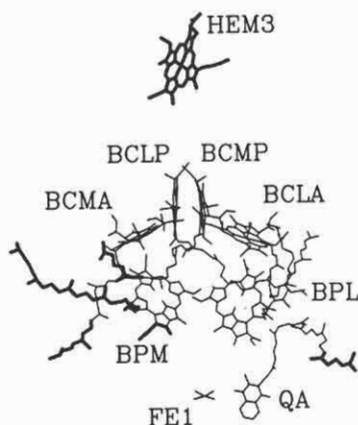


Fig. 1. Structure of chromophores in the simulated protein-segment together with their abbreviated names. Bonds between atoms inside the buffer region are denoted by thick solid lines.

The following calculations were carried out:

- We started the simulation, after minimizing the atomic coordinates provided by Deisenhofer and Michel according to CHARMM's energy function, with randomly chosen velocities conforming to physiological temperatures. The minimization and first simulation run allowed the reaction center segment to equilibrate for 20 ps to a state with relaxed sterical interactions.
- The second run, in the following referred to as run A, simulated for 20 ps the dynamics of the reaction center before the primary electron transfer. For this purpose the charge densities of the special pair bacteriochlorophylls and of the bacteriopheophytin in the functional branch was that of the neutral chromophores as determined by an MNDO<sup>6</sup> calculation. The motion resulting from run A had been analyzed.
- We then transferred an electron charge from the *special pair* to the bacteriopheophytin (BPL) by removing one electron from the highest occupied orbital of the *special pair* bacteriochlorophyll distant from the functional branch and depositing this electron into the lowest unoccupied orbital of the functional bacteriopheopytin. The corresponding charge densities of the chromophores were communicated to the CHARMM program.
- We then carried out a third simulation, in the following referred to as run B, which monitored the dynamics of the reaction center, thus perturbed, for 20 ps. The resulting motion was analyzed and compared with the behaviour before the electron transfer.
- Finally, we simulated an iron-depleted reaction center for 20 ps. We removed the iron-ion FE1 from our segment and investigated the resulting structural modifications.

### 3. RESULTS

#### Comparison of Average Structure from X-ray Data and Resulting from Molecular Dynamics Simulation

In order to test the molecular dynamics simulation in the light of available observations, we analyzed first structural changes occurring during the simulation. For this purpose we determined the average structure of run A and compared it to the X-ray data. The result is shown in Fig. 2. The mean differences in atomic positions between the molecular dynamics structure and the X-ray data is 1.05 Å. Most of the structure has remained remarkably stable during the dynamics before electron transfer (run A). However, the functional pheophytin group (BPL) and the phytol chains of the functional chromophores show larger structural changes indicating a higher degree of flexibility of these moieties than the other chromophores. Another structural deviation observed, namely that of the accessory bacteriochlorophyll of the non-functional branch (BCMA), might be explained by the fact that in our simulation we left out a carotenoid, which has been observed recently to lie close to BCMA<sup>7</sup>.

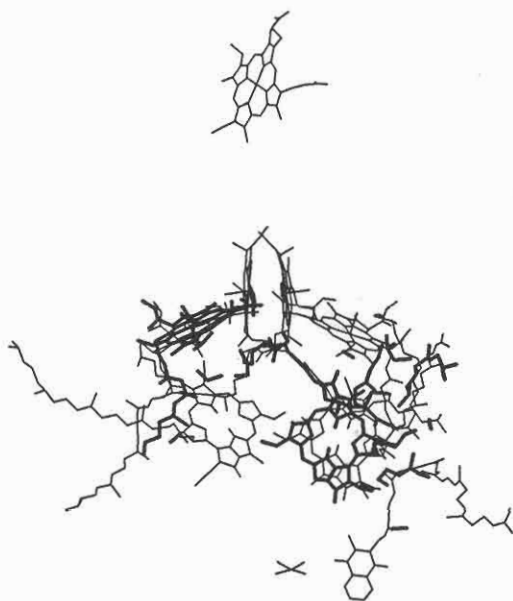


*Fig. 2. Comparison of dynamics and X-ray data. The average chromophore structure of run A is represented by thin lines. The X-ray structure is drawn by thick lines for those atoms the positions of which differ by more than 1.2 Å between the two structures.*

#### Thermal Motion

Thermal motion of the protein atoms induces fluctuations of the atomic positions  $\vec{r}_j$  around their equilibrium values  $\langle \vec{r}_j \rangle$ . The simplest measure of these fluctuations is given by the root mean square deviations  $\sigma_j = \sqrt{\langle (\vec{r}_j - \langle \vec{r}_j \rangle)^2 \rangle}$ ,  $\sigma_j$ , which can

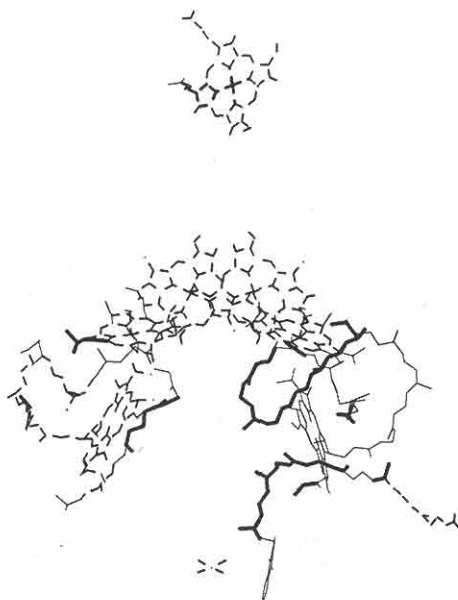


Fig. 3. Flexibility of chromophore atoms during run A. Dashed bonds are drawn between atoms whose root mean square deviations of the mean atomic position  $\sigma$  is less than  $0.4 \text{ \AA}$ , very flexible atoms ( $\sigma > 0.7 \text{ \AA}$ ) are connected by thick lines.

differ for different locations in the protein, provides a measure of the local flexibility of a protein. We have evaluated  $\sigma_j$  from run A separately for all atoms in the simulated reaction center segment.

The root mean square deviations of the chromophores during run A are illustrated in Fig. 3 : Dashed bonds are drawn between atoms that exhibit only a small degree of flexibility during run A, thick bonds denote atoms exhibiting a high degree of flexibility. The special pair ring structure turns out to be the most rigid part of the chromophore branches ( $\sigma < 0.3 \text{ \AA}$ ) . This rigidity might be important for the function of the *special pair* . The pheophytin ring and the phytol chains are found to be most flexible. The pheophytine BPL appears to be located in a small "pocket" inside the protein, which accounts for its mobility. The high flexibility might contribute to the different rates of forward- and backward electron transfer by allowing BPL to be shifted after primary electron transfer into a position unfavourable for the back-transfer.

As a second test for our calculations we compared the  $\sigma$  -values of all atoms with the root mean square values calculated from the temperature-factors (Debye-Waller-factors) of the X-ray analysis. The molecular dynamics  $\sigma$  -values are obtained as an average over a 20 ps time periode for a single protein. The X-ray temperature-factors involve an average over  $10^{20}$  molecules during several hours of observation time. The two sets of values, therefore, are strictly not equivalent. In fact, we would expect that the molecular dynamics  $\sigma$  -values are slightly smaller than the ones resulting from X-ray analysis. However, a comparison of the two sets of values may indicate how realistic the atomic fluctuations simulated by CHARMM actually are. For this purpose we compare in Figs. 4a,b the two sets of  $\sigma$  -values. Figure 4a shows the

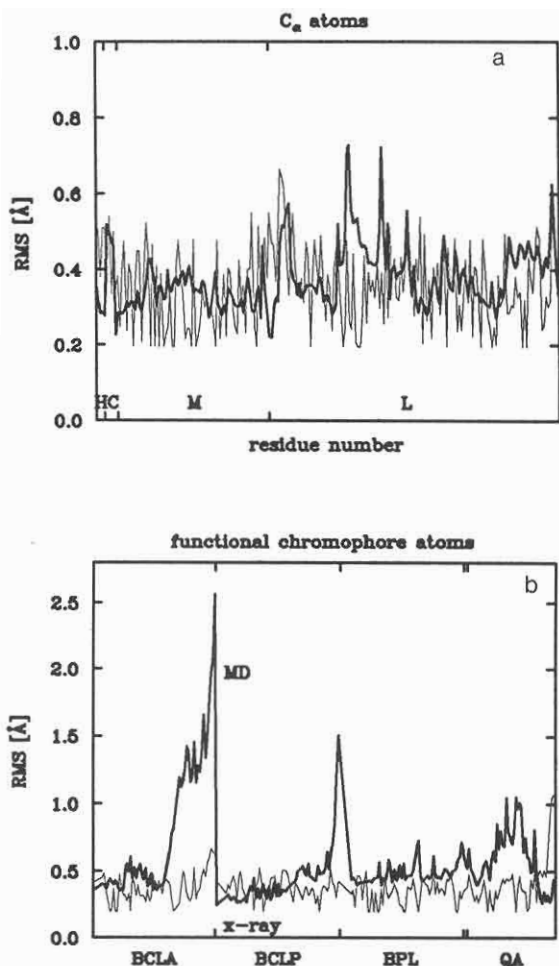


Fig. 4. Comparison of the root mean square deviations of the atomic positions as described by molecular dynamics simulation (run A) and as resulting from X-ray temperature-factors. Figure 4a compares the deviations for all  $C_{\alpha}$  atoms in the simulated protein segment, Fig. 4b compares the deviations for the atoms of some of the chromophores. Thick lines represent simulation data, thin lines data from X-ray analysis.

values for the  $C_{\alpha}$ -atoms, Fig. 4b the values for chromophore atoms. The simulated fluctuations of the  $C_{\alpha}$ -atoms as well as of the atoms belonging to the chromophore rings on the average compare rather well with the results from the X-ray analysis. Large differences can be observed, however, for atoms belonging to the phytol chains of BCLA and BCLP as well as to the chain of QA. The reason for these deviations might be due to faults in the simulation but it might also be due to false interpretation of the X-ray data<sup>8</sup>.

## Correlated Fluctuations

Another interesting measure of dynamical properties of the reaction center is furnished by the covariance  $C_{ik}$  between fluctuations of pairs of atoms  $i$  and  $k$ . This quantity is defined as

$$C_{ik} = \frac{c_{ik}}{\sqrt{c_{ii}c_{kk}}}$$

$$c_{ik} = \langle (\bar{r}_i - \langle \bar{r}_i \rangle) \cdot (\bar{r}_k - \langle \bar{r}_k \rangle) \rangle$$

Values of the covariance near +1 or -1 indicate that atomic motions are tightly coupled in phase (+1) or out of phase (-1), values around zero indicate a loose coupling.  $C_{ik}$  can differentiate between domains of the protein for which thermal fluctuations do not alter very much interatomic (inter-chromophore) distances ( $C_{ik} \approx 1$ ) from domains where thermal fluctuations lead to strong variations of these distances ( $C_{ik} \approx 0$ ).

Figure 5 provides results on the covariances between the *special pair* atoms (Fig. 5a) and between the atoms belonging to BCLP and BPL (Fig. 5b). Figure 5a illustrates that there exists a high degree of covariance for the motions of the two bacteriochlorophyll rings. This implies that the rings form a sandwich complex and move in phase. In contrast, the motions of the two special pair phytol chains are rather uncorrelated with the motion of the rings and are also uncorrelated with each other. Figure 5b shows on the other hand that the motion of the phytol chain of one of the *special pair* chlorophylls (BCLP) is strongly coupled in phase to the pheophytine (BPL) ring. This dynamic coupling, essentially an intermolecular attraction, could provide the interaction needed for the photo-induced primary electron transfer between the special pair and BPL in case the transfer involves the BCLP phytol chain. This attraction would prevent any thermal motion from impeding the fast (3 ps) primary electron transfer.

We have also investigated the covariance between motions of the remaining chromophores. The chromophores consecutive along the electron transfer route BCMP, (BCLA ?), BPL, QA are coupled pairwise in phase, i.e. BCMP to BCLA, BCLA to BPL . . . . This implies that thermal fluctuations do not affect very much the relative distances between these chromophores. This could indicate that the chromophore arrangement is optimized for the electron (forward) transfer and that structural disturbances due to the inherent thermal mobility are kept at a minimum. This feature obviously can have important implications for the mechanism of primary electron transfer: edge to edge couplings between the chromophores, which without this feature may be unreliable due to thermal motions, might have been tuned to rather precise values in the reaction center to provide a most effective forward electron transfer, i.e. along the lines suggested by Plato, Fischer and others in this workshop.

## Response to Electron Transfer

We want to investigate now in how far structural and dynamical properties of the reaction center change when an electron charge is suddenly moved from the *special pair* to the functional bacteriopheophytine. For this purpose we have compared the motion of the reaction center monitored during run A before the transfer with the motion monitored during run B after the electron transfer. The simulations showed that the electron transfer disturbs the protein structure.

In Fig. 6 we present the average structure of run B. The mean structural difference to the average structure of run A is found to be 0.32 Å. For atoms whose position has changed by more than 0.4 Å the average structure of run A is also displayed in Fig. 6. The largest structural differences occur for the pheophytine BPL and the (phytol) chains. After the electron is transferred, BPL is shifted towards the *special*

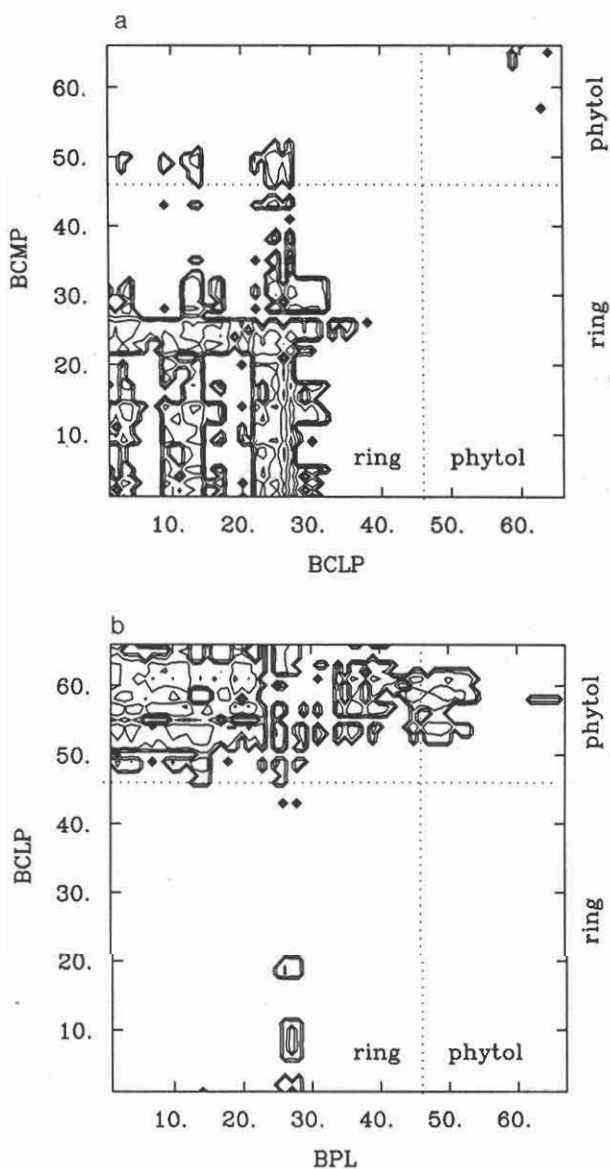


Fig. 5. Covariance of chromophores. Figure 5a displays the covariances  $C_{ik}$  between the special pair atoms and Fig. 5b the covariances between the atoms of BCLP and BPL. The axes present the atomic labels  $i$  and  $k$ . All correlations  $C_{ik}$  are positive. The blank area denotes pairs of atoms  $i, k$  with correlations smaller than 0.3. Figure 5 shows further the contour lines which separate regions with larger correlations; the contour lines correspond to increments of 0.1.

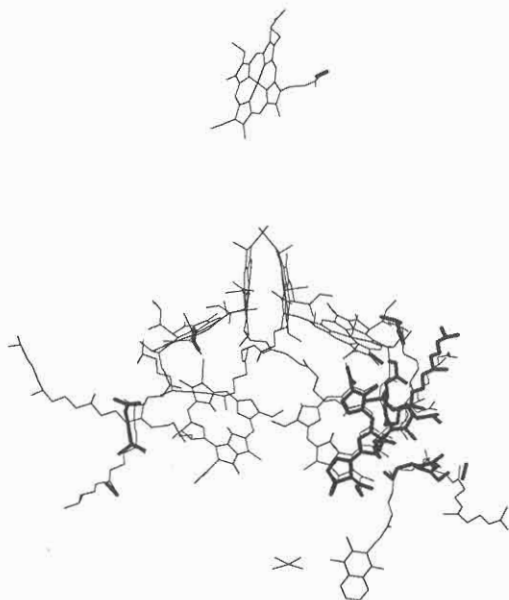


Fig. 6. Structural differences induced by primary electron transfer. The average structure of run B is represented by thin lines. The average structure of run A is overlaid by thick lines for those atoms the positions of which differ between the two structures by more than  $0.4 \text{ \AA}$ .

pair. This motion is induced by the additional Coulomb interaction between the (after the electron transfer) positively charged special pair and the negatively charged pheophytine. As already mentioned above this might hinder the backtransfer of the electron by altering the alignment of the chromophores BCMP, BCLA, BPL or the tight interaction of BPL with the BCLP phytol chain. We will discuss this issue in more detail in a second contribution to this workshop, concerning electrostatic properties of the reaction center<sup>5</sup>. The degree of mobility (flexibility as measured by  $\sigma_j$ ) does not alter very much after electron transfer except that BPL becomes somewhat less flexible. This decrease in flexibility might be due to BPL being shifted into a cleft inside the reaction center. The existence of a cleft-like pocket is indicated by the shape of BPL as well as by the fact that our simulations also showed significant differences for the BPL location compared to the location observed through X-ray scattering. It is possible that this pocket inside the L subunit furnishes some degree of control during the primary electron transfer by altering the chromophore - chromophore interactions through the resulting mobility and also allowing for fast and effective dielectric relaxation (see also Ref. 5).

### Iron Depleted Reaction Center

In order to elucidate how the amino acid, Fe, and chromophore composition of the reaction center controls structure, dynamics and function one may modify the reaction center. For an unequivocal interpretation of such experiments the modifications need to be very specific. Currently it is attempted to modify the photosynthetic reaction center of *Rps. viridis* by genetic engineering methods (site directed mutagenesis). We expect that molecular dynamics simulations will play an important role in this respect in suggesting amino acid replacements as well as in interpreting the effects of

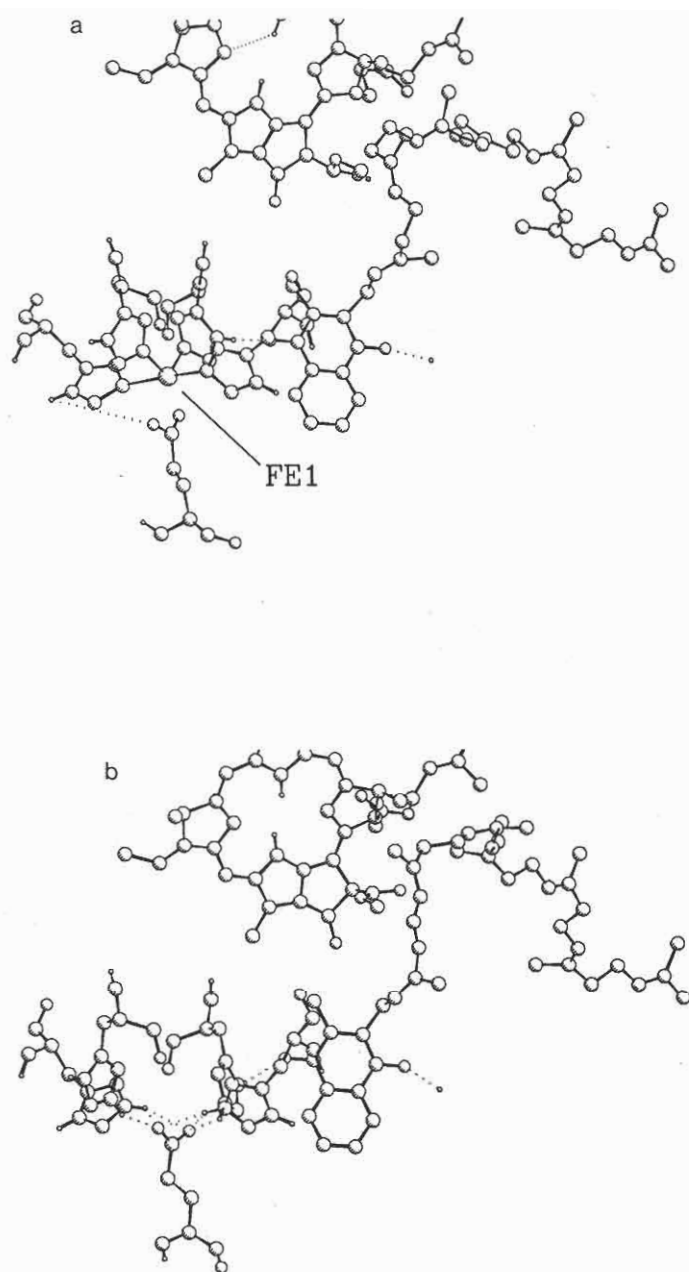


Fig. 7. Structural differences induced by iron depletion. The site of iron FE1 for the native (X-ray) structure is shown in Fig. 7a. Part of the tetrapyrrol-ring of BPL is seen near the top and the menaquinone QA with its phytol chain is seen on the right side of the diagram. The iron-ion is bonded to four histidine groups shown on the left side as well as to a glutamate (M232) seen near the bottom. Hydrogen bonds are represented by dashed lines. Fig. 7b displays the same region for the iron depleted reaction center.

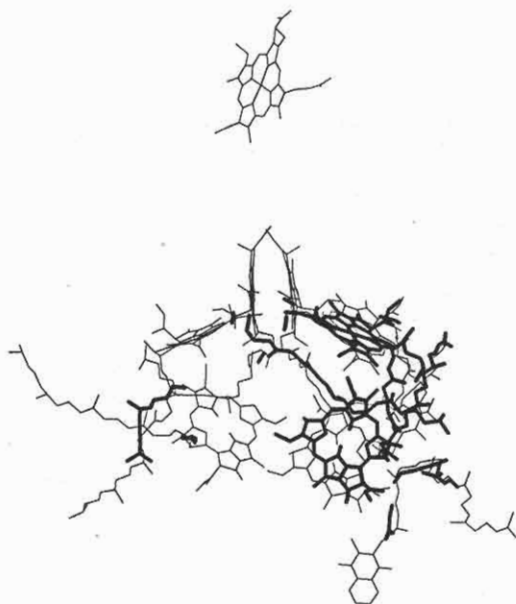


Fig. 8. Structural differences between the iron-depleted and the native reaction center. Thin lines represent the average structure resulting from a simulation of the iron depleted reaction center, thick lines represent the native structure (average structure from run A) for atoms which differ in their positions between the two structures by more than  $0.7 \text{ \AA}$ .

such replacements. As a first attempt in this direction we consider in this contribution the effect of iron depletion on the structure of the photosynthetic reaction center.

Iron-depleted reaction centers have been prepared and examined in the case of the *Rps. sphaeroides* reaction center<sup>9,10</sup>. The main effects observed in this case after iron depletion was a decrease in the yield of the electron transferred to the quinone QA from 100% to 47% and a 20-fold increased lifetime of the negatively charged BPL. The native behaviour could be restored by reconstitution with several metal ions. These results are somehow surprising since the iron-ion is located far away from BPL. The authors<sup>9,10</sup> suggest mainly three possible explanations: (i) structural rearrangements, (ii) alteration of the electrostatic potential and (iii) change of vibronic couplings. In order to understand the effect of iron depletion we simulated the photosynthetic reaction center of *Rps. viridis* without the iron FE1. Because of the close structural similarities between the reaction centers of *Rps. sphaeroides* and *Rps. viridis*<sup>11</sup> we assume that iron depletion may have similar effects on the latter and, hence, our simulation might contribute to an explanation of the effect of iron depletion on the former reaction center.

The simulation has been carried out in the following way. First, we removed the iron FE1 from the simulated segment of the reaction center. Second, we minimized the energy by relaxing the atomic coordinates. Third, we carried out a 30 ps simulation to allow further relaxation of the altered protein. After this we performed finally a 21 ps simulation which was then analyzed.

In Fig. 7 we present the structural differences near the location of FE1. Figure 7a displays the native structure with the iron present. The iron is shown bonded to four histidine groups. Hydrogen bonds are represented by dashed lines. Also a glutamate

(M232) can be seen near the iron as well as, further away, the menaquinone (QA) and part of the bacteriopheophytin (BPL). The same region is shown for the iron-depleted reaction center in Fig. 7b. The important change which occurs at the site of FE1 is that glutamate M232 substitutes for the missing iron-ion forming hydrogen bonds to the four histidines. As a result the local structures at the FE1 site in the native and iron-depleted protein are very similar. However, a further analysis showed that compared to the native structure the two protein subunits L and M in the iron-depleted reaction center are shifted slightly with respect to each other. This shift changes the arrangement of chromophores in the reaction center as shown in Fig. 8.

The average chromophore arrangement resulting from the simulation of the iron-depleted reaction center is compared in Fig. 8 to the average structure which resulted from run A describing the native reaction center (see above). The mean difference of the atomic positions in the two structures is 0.79 Å. One notices in Fig. 8 that the orientations of BCLA and BPL are very much disturbed. It appears that the iron is needed as a glue between the L and M subunits of the photosynthetic reaction center which also keeps the chromophores in their proper arrangement. The fact that iron depletion has a profound effect on the reaction center quantum yield<sup>9,10</sup> in connection with our findings hints again at the importance of the proper relative arrangement of the chromophores for an effective primary electron transfer process in the reaction center.

#### ACKNOWLEDGEMENTS

The authors like to thank Zan Schulten for advice and help. This work has been supported by the Deutsche Forschungsgemeinschaft (SFB 143-C1) and by the National Center of Supercomputer Applications in Urbana, IL.

#### REFERENCES

1. J. Deisenhofer, O. Epp, K. Miki, R. Huber, H. Michel, X-ray Structure Analysis of a Membrane Protein Complex J Molec Biol 180:385 (1984)
2. J. Deisenhofer, O. Epp, K. Miki, R. Huber, H. Michel, Structure of the protein subunits in the photosynthetic reaction center of *Rhodospseudomonas viridis* at 3 Å resolution, Nature 318:618 (1985)
3. B. R. Brooks et al., CHARMM: A Program for Macromolecular Energy Minimization, and Dynamics Calculations, J Comp Chem 4:187 (1983)
4. C. L. Brooks, A. Brünger, M. Karplus, Active Site Dynamics in Protein Molecules: A Stochastic Boundary Molecular-Dynamics Approach, Biopolymers 24:843 (1985)
5. H. Treutlein et al., Electrostatic control of electron transfer in the photosynthetic reaction center of *Rps. viridis*, contribution to this workshop
6. Dewar Group, University of Texas at Austin, Austin, TEXAS 78712
7. J. Deisenhofer's contribution to this workshop
8. J. Kuriyan et al., Effect of anisotropy and anharmonicity on protein crystallographic refinement, J Molec Biol 190:227 (1986)
9. C. Kirmaier et al., Primary photochemistry of iron-depleted and zinc-reconstituted reaction centers from *Rps. sphaeroides*, PNAS 83:6407 (1986)
10. R. J. Debus, G. Feher, M. Y. Okamura, Iron-depleted Reaction Centers from *Rps. sph. R-26.1*: Characterization and Reconstitution with  $Fe^{2+}$ ,  $Mn^{2+}$ ,  $Co^{2+}$ ,  $Ni^{2+}$ ,  $Cu^{2+}$  and  $Zn^{2+}$ , Biochemistry 25:2276 (1986)
11. J. P. Allen et al., Structural homology of reaction centers from *Rps. sph.* and *Rps. v.* as determined by X-ray diffraction, PNAS 83:8589 (1986)